

Electromagnetically induced transparency with an ensemble of donor-bound electron spins in a semiconductor

Maksym Sladkov,¹ A. U. Chaulal,¹ M. P. Bakker,¹ A. R. Onur,¹ D. Reuter,² A. D. Wieck,² and C. H. van der Wal¹

¹Zernike Institute for Advanced Materials, University of Groningen, NL-9747AG Groningen, The Netherlands

²Angewandte Festkörperphysik, Ruhr-Universität Bochum, D-44780 Bochum, Germany

(Received 6 July 2010; revised manuscript received 4 September 2010; published 24 September 2010)

We present measurements of electromagnetically induced transparency with an ensemble of donor-bound electrons in low-doped *n*-GaAs. We used optical transitions from the Zeeman-split electron-spin states to a bound trion state in samples with optical densities of 0.3 and 1.0. The electron-spin dephasing time $T_2^* \approx 2$ ns was limited by hyperfine coupling to fluctuating nuclear spins. We also observe signatures of dynamical nuclear polarization but find these effects to be much weaker than in experiments that use electron-spin resonance and related experiments with quantum dots.

DOI: 10.1103/PhysRevB.82.121308

PACS number(s): 78.47.jh, 71.55.Eq, 42.50.Gy, 71.35.Pq

A localized electronic spin in a semiconductor is a promising candidate for implementing quantum information tasks in solid state. Optical manipulation of single-electron and single-hole systems has been realized with quantum dots^{1–5} and by using donor atoms that are not ionized at low temperature (D^0 systems).^{6–8} These results illustrate the potential of quantum-optical control schemes that come within reach when adapting techniques from the field of atomic physics. An advantage of the D^0 systems over dots is that these can be operated as an ensemble with very little inhomogeneity for the optical transition energies. Such ensembles at high optical density are key for robust quantum-optical control schemes that have been designed for preparing nonlocal entanglement between spins, quantum communication, and applying strong optical nonlinearities.^{9,10} A critical step toward implementing these schemes is the realization of electromagnetically induced transparency (EIT). We present here measurements of EIT with an ensemble of donor-bound electron spins in low-doped *n*-GaAs, in samples with optical densities of 0.3 and 1.0.¹¹ We build on an earlier indirect observation of coherent population trapping with this system.⁶ Extending this to a direct realization of EIT with an optically dense medium is essential for getting access to strong field-matter interactions without using optical cavities and for the application and study of transmitted signal fields.^{9,10}

We implemented EIT in its most typical form where a spin-up and a spin-down state ($|\uparrow\rangle$ and $|\downarrow\rangle$ of the electron in the D^0 system) have an optical transition to the same excited state $|e\rangle$ [Fig. 1(e)]. We Zeeman split the states $|\uparrow\rangle$ and $|\downarrow\rangle$ with an applied magnetic field. For the state $|e\rangle$ we used the lowest energy level of a donor-bound trion system [D^0X with two electrons in a singlet state and a spin-down hole with $m_h = -\frac{1}{2}$ (Ref. 8) localized at the donor site]. EIT is then the phenomenon that absorption by one of the optical transitions is suppressed because destructive quantum interference with the other transition prohibits populating the state $|e\rangle$. The D^0 systems are then trapped in a dark state that is in the ideal case a coherent superposition of the states $|\uparrow\rangle$ and $|\downarrow\rangle$ only.^{6,11} This state is proportional to $\Omega_c|\uparrow\rangle - \Omega_p|\downarrow\rangle$ with Ω_c and Ω_p the Rabi frequencies of the control and probe field that drive the two transitions.¹⁰

We present results of implementing EIT in GaAs, and we

studied the interactions between the solid-state environment and driving EIT. In particular, the D^0 systems have a single electron in a hydrogenlike $1s$ wave function with a Bohr radius of ~ 10 nm and each electron spin has hyperfine coupling to $\sim 10^5$ fluctuating nuclear spins. We studied how this limits the electron-spin dephasing time and how driving EIT can result in dynamical nuclear polarization (DNP). In addition, we find that it is crucial to suppress heating effects from the nearby free exciton resonance, and demonstrate that with direct heat sinking of GaAs layers EIT can be driven with $\Omega_c/2\pi$ up to 2 GHz, while keeping the spin dephasing time $T_2^* \approx 2$ ns near the level that results from the nuclear-spin fluctuations.

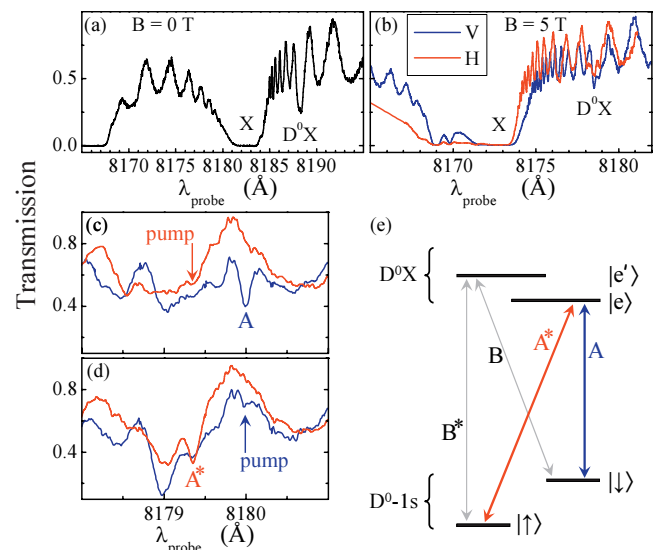


FIG. 1. (Color) (a) Transmission spectroscopy at $B=0$ T. (b) Transmission at $B=5.0$ T for H and V polarization. (c) Pump-assisted spectroscopy with H-polarized pumping at the A^* transition shows enhanced absorption for the A transition for the scan with a V-polarized probe (blue trace) but not with an H-polarized probe (red trace). (d) Complementary to (c), V-polarized pumping at A shows enhanced absorption for the A^* transition with an H-polarized probe. (e) Energy levels and optical transitions of the D^0 - D^0X system.

We used epitaxially grown GaAs films of 10 μm thickness with Si doping at $n_{\text{Si}}=3 \times 10^{13}$ and $1 \times 10^{14} \text{ cm}^{-3}$. At these concentrations the wave functions of neighboring donor sites do not overlap, which yields an ensemble of noninteracting D^0 systems. The films were transferred to a wedged sapphire substrate with an epitaxial lift-off process¹² and fixed there by van der Waals forces which assures high heat sinking. The sapphire substrate was mounted on the copper cold finger of a bath cryostat (4.2 K) in the center of a superconducting magnet with fields B up to 8 T in the plane of the sample (z direction). Laser light was brought to the films at normal incidence (Voigt geometry) via a polarization-maintaining single-mode fiber. The two linear polarizations supported by the fiber are set parallel (V polarization) and orthogonal (H polarization) to the applied magnetic field. The V polarization can drive π transitions (no change in z -angular momentum) and the H polarization can drive transitions with a change in z -angular momentum of $\pm\hbar$.

Two cw Ti:sapphire lasers (Coherent MBR-110, linewidth below 1 MHz) provided tunable probe and control fields. Focusing in the sample volume was achieved with a piezomotor controlled confocal microscope. During transmission experiments we defocused the microscope to a spot of $\sim 16 \mu\text{m}$ diameter to avoid interference effects from the cavity that is formed between the sample surface and the facet of the fiber. The probe field was amplitude modulated at 6 kHz and we used lock-in techniques for detecting light that is transmitted through the sample with a photodiode directly behind the sample. The signal due to unmodulated control field is rejected by ac coupling of the measurement electronics.

We first report transmission experiments that identify the spectral position of the D^0X related resonances. Only the probe laser was used. Figure 1(a) shows a spectrum taken at $B=0$ T (identical result for H and V polarization) and Fig. 1(b) shows a result for $B=5.0$ T with a separate trace for H and V polarization. The strong absorption labeled X is due to excitation of free excitons. Resonant absorption by donor-bound excitons (D^0X) occurs at 8187.5 \AA for $B=0$ T and at 8179.5 \AA for $B=5.0$ T. The shift of the resonances with magnetic field is the diamagnetic shift. The spacing of 5 \AA between the X and D^0X resonances is in good agreement with previously reported binding energies.^{13,14} The oscillating background superimposed on the resonances is due to a Fabry-Perot effect in the GaAs film and its chirped wavelength dependence around X is due to the wavelength-dependent refractive index that is associated with the strong free exciton absorption.

For identifying the A and A^* transitions of Fig. 1(e) within the fine structure of D^0X spectra at high fields we performed scanning-probe laser spectroscopy while the control laser is applied for optical pumping of a particular D^0X transition (this also eliminates bleaching by the probe). Figure 1(c) shows spectra obtained with pumping at A^* (8179.3 \AA) with H polarization. This leads to enhanced absorption at the A resonance (8180.0 \AA) for the probe scan with V polarization. The complementary experiment with pumping V-polarized light into this A transition leads to enhanced absorption of H-polarized light at transition A^* [Fig. 1(d)]. We could also perform such cross-pumping experiments using

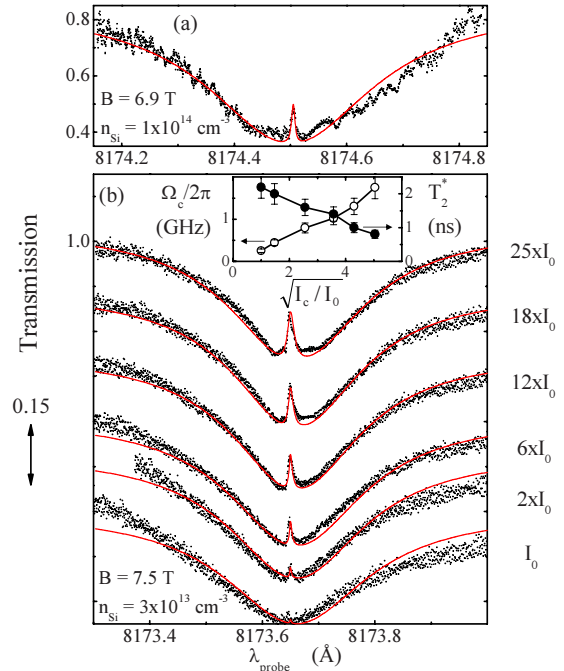


FIG. 2. (Color online) (a) EIT spectrum from sample with Si doping at $1 \times 10^{14} \text{ cm}^{-3}$. Dots—experiment. Line—numerical fit. (b) EIT spectra from sample with Si doping at $3 \times 10^{13} \text{ cm}^{-3}$, for probe-field intensity 0.04 W cm^{-2} and a range of control-field intensities I_c with $I_0=0.4 \text{ W cm}^{-2}$. The inset shows the fitting results for Rabi frequency Ω_c and spin dephasing time T_2^* .

the B and B^* transitions to the level $|e'\rangle$ [the first excited state of the series of energy levels of the D^0X complex, see Fig. 1(e)]. We thus confirmed that the pair of transitions labeled as A and A^* address a so-called closed three-level Λ system and that this is the pair with lowest energies within the D^0X resonances. This interpretation is also consistent with the polarization dependence of these transitions.^{6,14} In the field range 5–8 T, the A and A^* transitions are spectrally well separated from the transitions B, B^* , and transitions to higher excited states of the D^0X complex. The observed D^0 Zeeman splitting corresponds to an electron g factor $|g|=0.42$ and also agrees with previous reports.^{6,14}

We now turn to the observation of EIT (Fig. 2). For these results we fixed the control laser central on the A transition (V polarization) while the probe laser is scanned across the A^* transition (H polarization). When the control and probe field meet the condition for two-photon Raman resonance (the difference in photon energy exactly matches the D^0 spin splitting), a narrow peak with enhanced transmission appears inside the broader A^* absorption dip, which is the fingerprint of EIT. In Fig. 2(a) this occurs inside an A^* absorption with optical density 1.0 while for the sample with $n_{\text{Si}}=3 \times 10^{13} \text{ cm}^{-3}$ this is 0.3 [Fig. 2(b)]. We further focus on this latter sample since higher resolution of the EIT spectra makes it more suited for our further studies.

The lines in Figs. 2 and 3 are results of fitting EIT spectra with the established theory.¹⁰ This involves calculating the steady-state solution of a density-matrix equation for the three-level system, and accounts for coherent driving by the lasers and relaxation and dephasing rates between the levels.

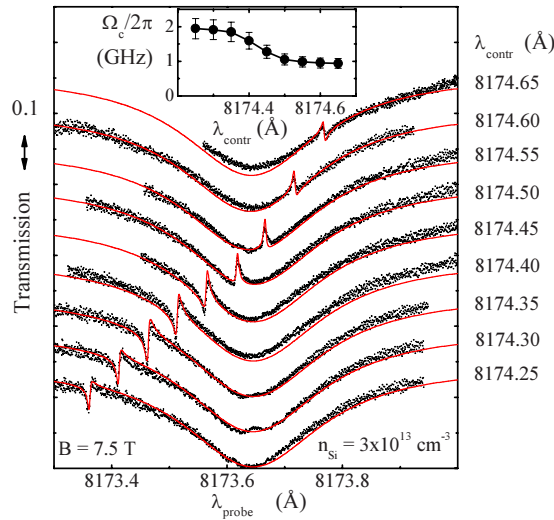


FIG. 3. (Color online) Dependence of EIT spectra on control-field detuning. The position of the EIT peak follows precisely the control-field detuning from transition A. Dots—experiment with control (probe) intensity $6(0.04) \text{ W cm}^{-2}$. Lines—fits with $T_2^* = 2 \text{ ns}$ and Ω_c as presented in the inset.

The free parameters are the inhomogeneous broadening γ_{A^*} (typically 6 GHz) for the optical transition A^* , the spin dephasing time T_2^* and the control-field-induced Rabi frequency Ω_c (and $\Omega_p \ll \Omega_c$). The rest of the parameters are the same as in Ref. 6 and we found Ω_c always consistent with an independent estimate from the optical intensity and electric dipole moment. We obtain good fits and the main features in our results are consistent with EIT, as we discuss next.

Figure 2(b) shows EIT spectra taken at different intensities I_c of the control field, where a stronger control field yields a higher and broader EIT peak. As expected for EIT, we observe that Ω_c from fits scales linearly with $\sqrt{I_c}$ [Fig. 2(b), inset]. The Ω_c values reach $2\pi \times 2 \text{ GHz}$ and we could only obtain clear EIT spectra with such high Ω_c in samples with complete adhesion onto the sapphire substrate. Our results from samples with incomplete adhesion (and work with epilayers that are not removed from the original GaAs substrate^{6–8}) suffer from heating, which is observed as a broadening of the free exciton line into the region of the D^0X resonances. The values of T_2^* that we find in our experiments are discussed below.

Figure 3 shows how the EIT peak position depends on detuning of the control field from the A transition. As expected, the EIT peak follows the detuning of the control field. However, the EIT peak in the blue-detuned traces is clearly more prominent than in the red-detuned cases. We attribute this to a change in the effective Rabi frequency Ω_c that results from the weak Fabry-Perot interference within the GaAs film, and we can indeed fit the results with fixed $T_2^* = 2 \text{ ns}$ and varying Ω_c (Fig. 3, inset). We can exclude that the difference in the quality of EIT spectra is coming from optical coupling to a level outside our Λ system since all other transitions are well separated spectrally and in polarization dependence [e.g., the B and B^* transitions, see Fig. 1(e)].

An important topic that needs to be addressed next with this realization of EIT concerns the influence of the hyperfine coupling between each electron spin and $\sim 10^5$ nuclear spins. A polarization of the nuclear spins acts on the electron spin as an effective magnetic field B_{nuc} . The average polarization affects the Zeeman splitting, and this can be directly observed in EIT spectra as a red (blue) shift of the EIT peak for a reduced (enhanced) Zeeman splitting. The nuclear-spin fluctuations around the average dominate via this mechanism the inhomogeneous electron-spin coherence time T_2^* . This is a key parameter for the shape of the EIT peak (longer T_2^* gives a sharper peak) and the magnitude of these fluctuations can therefore be derived from the EIT spectra as well. At our fields and temperature nuclear spins are in equilibrium close to full random orientation. The expected value for T_2^* for this case is $\sim 2 \text{ ns}$,^{6,15} and is in agreement with the values that we observe.

The hyperfine coupling can also result in DNP, which is the transfer of angular momentum from the electron to the nuclear spins when the electron spin is driven out of equilibrium. Earlier experiments on our type of D^0 system with microwave-driven electron-spin resonance (ESR) (Ref. 15) and optical experiments on quantum dots showed strong DNP.^{3,4} In both cases the effects were so strong that it gave an unstable resonance condition for tuning at ESR and EIT (the systems trigger a DNP cycle that drives them out of resonance). DNP can also result in a suppression of the nuclear-spin fluctuations, which yields a longer T_2^* .^{2–4,16} Our experiment, however, only shows weak DNP. We never observed a significant change in the Zeeman energy (as derived from subtracting the probe and control photon energies at the EIT peak) from the EIT driving itself. We only observed in several data sets a moderate EIT peak narrowing over the course of a few hours of data taking (at fixed settings of the EIT parameters). In order to confirm the role of nuclear spins we carried out various attempts to induce stronger DNP effects.

An example of the strongest DNP effects that we could induce is presented in Fig. 4. Here we first applied strong driving of the A^* transition for 30 min with an intensity equivalent to a Rabi frequency of $2\pi \times 10 \text{ GHz}$. This pumps the system fully into $|\downarrow\rangle$. After pumping we take fast “snapshots” of the EIT peak (50 s A^* scans, $\Omega_p/2\pi = 25 \text{ MHz}$, and control at A with $\Omega_c/2\pi = 1 \text{ GHz}$). Between scans we kept the system in the dark for 10 min. Figure 4 shows six subsequent snapshots. Right after pumping we observe a blue-shifted and sharpened EIT peak ($T_2^* = 3 \text{ ns}$). This enhancement of T_2^* probably results from suppressed nuclear-spin fluctuations, which generally occurs when the polarization gets squeezed between a polarizing and depolarizing mechanism with rates that are both enhanced due to the DNP.^{3,4,16} The peak shift agrees in sign with Ref. 15 but corresponds to $B_{\text{nuc}} = 21 \text{ mT}$ only (the ESR studies¹⁵ and the work on dots easily induced 200 mT–1 T). Subsequent spectra show a clear broadening of the EIT peak, which also shifts back to the red. After about 1 h, T_2^* (Fig. 4, inset) and the peak position stabilize at the values that were observed before pumping. This agrees with the relaxation time for DNP with

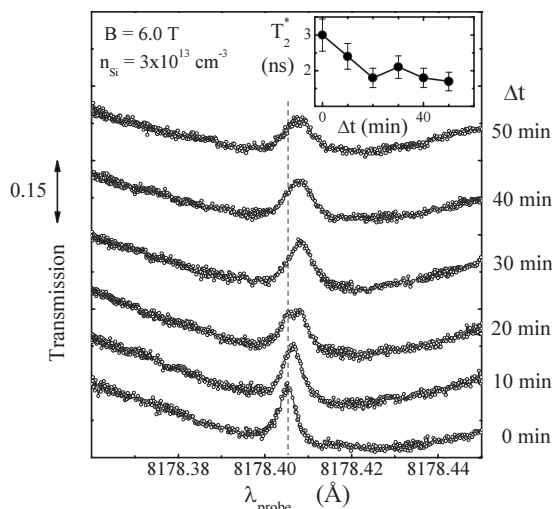


FIG. 4. Evolution of the EIT peak after 30 min pumping of the A^* transition. Fast EIT snapshots were taken at 10 min intervals during which the sample was kept in the dark. The dashed line is a guide for showing the shift in peak position. The inset presents fitting results that show the change in T_2^* .

D^0 systems.¹⁵ Upon exploring how DNP occurs for various EIT and pump conditions we found the effects to be too weak for systematic control and drawing further conclusions, and full understanding goes beyond the scope of the present

work. The work with dots showed that the mechanism that dominates the DNP rate can be complex and needs to account for driving-field-assisted processes.^{3,4} We can nevertheless conclude that our spin dephasing time is indeed limited by coupling to nuclear spins.

In conclusion, we presented direct evidence that a D^0 ensemble in GaAs can be operated as a medium for EIT. The electron-spin dephasing time limits the quality of the EIT and is in the range $T_2^* \approx 2$ ns that results from hyperfine coupling to fluctuating nuclear spins. The EIT spectra form a sensitive probe for detecting how DNP changes the fluctuations and the average of nuclear-spin polarization. However, direct optical driving of D^0 transitions yields much weaker DNP effects than in electron-spin-resonance experiments with D^0 systems and related EIT experiments on quantum dots and a complete physical picture of DNP effects in our system is not available. Still, initial signatures of controlled DNP effects show that the electron-spin dephasing time can be prolonged. Our experimental approach is suited for exploring this further in conjunction with experiments that aim to implement various applications of EIT.^{9,10}

We thank B. Wolfs, J. Sloot, and S. Lloyd for contributions, and the Dutch NWO and FOM, and the German programs DFG-SPP 1285, BMBF nanoQUIT and Research school of Ruhr-Universität Bochum for support.

¹D. Press, T. D. Ladd, B. Zhang, and Y. Yamamoto, *Nature (London)* **456**, 218 (2008).

²A. Grelich, S. E. Economou, S. Spatzek, D. R. Yakovlev, D. Reuter, A. D. Wieck, T. L. Reinecke, and M. Bayer, *Nat. Phys.* **5**, 262 (2009).

³X. Xu, W. Yao, B. Sun, D. G. Steel, D. Gammon, A. S. Bracker, and L. J. Sham, *Nature (London)* **459**, 1105 (2009).

⁴C. Latta *et al.*, *Nat. Phys.* **5**, 758 (2009).

⁵D. Brunner *et al.*, *Science* **325**, 70 (2009).

⁶Kai-Mei C. Fu, C. Santori, C. Stanley, M. C. Holland, and Y. Yamamoto, *Phys. Rev. Lett.* **95**, 187405 (2005).

⁷K. M. C. Fu, S. M. Clark, C. Santori, C. R. Stanley, M. C. Holland, and Y. Yamamoto, *Nat. Phys.* **4**, 780 (2008).

⁸S. M. Clark, Kai-Mei C. Fu, Q. Zhang, T. D. Ladd, C. Stanley, and Y. Yamamoto, *Phys. Rev. Lett.* **102**, 247601 (2009).

⁹L. M. Duan, M. D. Lukin, J. I. Cirac, and P. Zoller, *Nature*

(London) **414**, 413 (2001).

¹⁰M. Fleischhauer, A. Imamoglu, and J. Marangos, *Rev. Mod. Phys.* **77**, 633 (2005).

¹¹T. Wang, R. Rajapakse, and S. F. Yelin, *Opt. Commun.* **272**, 154 (2007).

¹²E. Yablonovitch, T. Gmitter, J. Harbison, and R. Bhat, *Appl. Phys. Lett.* **51**, 2222 (1987).

¹³E. Bogardus and H. Bebb, *Phys. Rev.* **176**, 993 (1968).

¹⁴V. A. Karasyuk, D. G. S. Beckett, M. K. Nissen, A. Villemaire, T. W. Steiner, and M. L. W. Thewalt, *Phys. Rev. B* **49**, 16381 (1994).

¹⁵T. A. Kennedy, J. Whitaker, A. Shabaev, A. S. Bracker, and D. Gammon, *Phys. Rev. B* **74**, 161201 (2006).

¹⁶I. T. Vink, K. C. Nowack, F. H. L. Koppens, J. Danon, Y. V. Nazarov, and L. M. K. Vandersypen, *Nat. Phys.* **5**, 764 (2009).